horticulturae

MDPI

Article

Tobacco Straw Biochar Mitigates Cadmium Accumulation in Amaranth (*Amaranthus tricolor* L.): A Cultivar-Specific Response

Jie Li [1], Shudong Zhou [1], Zuxuan Min [1], Gaoyi Dong [1], Yanling Li [1], Minghua Deng [2], Jingxia Gao [3,*] and Jingyuan Zheng [1,*]

[1] Institute of Vegetables, Hunan Academy of Agricultural Sciences, Changsha 410125, China; licky0725@126.com (J.L.); zhoushudong@hunaas.cn (S.Z.); minzuxuan1214@126.com (Z.M.); donggaoyi0524@126.com (G.D.); liyanling0011@126.com (Y.L.)
[2] College of Landscape and Horticulture, Yunnan Agricultural University, Kunming 650201, China; dengminghua2013@sina.com
[3] Ningxia Academy of Agriculture and Forestry Sciences, Yinchuan 750002, China
* Correspondence: gjj830114@163.com (J.G.); zhengjingyuan2004@hunaas.cn (J.Z.)

Abstract

Cadmium (Cd) contamination in agricultural soils poses a severe threat to food safety and human health through the food chain. This study investigated the efficacy of tobacco straw-derived biochar, applied at varying rates (0%, 1%, 2%, and 5% *w*/*w*), in mitigating Cd accumulation and modulating the growth and nutritional quality of two amaranth (*Amaranthus tricolor* L.) cultivars (red and green) grown in Cd-contaminated soil (initial total Cd of 2.18 mg/kg). The pot experiment revealed that biochar significantly reduced Cd uptake in both cultivars. Mechanistically, biochar elevated soil pH and drove the in-situ transformation of highly bioavailable exchangeable Cd into the more stable Fe-Mn oxide-bound fraction. Consequently, shoot Cd concentrations were notably suppressed, with the red cultivar exhibiting a superior response; the 2% biochar treatment optimally reduced its shoot Cd concentration by 37.6% compared to the control. Crucially, the amendments induced highly cultivar-specific growth responses. While biochar application simultaneously mitigated Cd toxicity and promoted biomass accumulation in red amaranth (yielding a 58.6% increase in shoot dry weight at the 2% rate), it exerted antagonistic, inhibitory effects on the growth of green amaranth. In conclusion, the incorporation of 2% tobacco straw biochar serves as a highly effective, dual-purpose strategy for significantly reduced health risks and enhancing the yield of red amaranth in Cd-contaminated fields. However, in green amaranth, biochar application induced a physiological trade-off, inhibiting growth despite successful Cd reduction. Furthermore, while Cd concentrations were significantly reduced on a dry-weight basis, future evaluations based on fresh-weight regulatory limits are required to fully confirm food safety.

Keywords: agricultural residue valorization; leafy vegetables; cadmium immobilization; food safety; genotypic variation; soil remediation

Check for updates

Academic Editor: Yanyou Wu

Received: 22 April 2026
Revised: 18 June 2026
Accepted: 29 June 2026
Published: 2 July 2026

Copyright: © 2026 by the authors. Licensee MDPI, Basel, Switzerland. This article is an open access article distributed under the terms and conditions of the Creative Commons Attribution (CC BY) license.

1. Introduction

Soil pollution has emerged as a critical global issue, posing a severe threat to food security and human health through the food chain. Among agricultural contaminants, the heavy metal cadmium (Cd) is of particular concern due to its high mobility and bioavailability in soils. It is readily absorbed and accumulated by crops, subsequently entering the human diet. Prolonged dietary exposure to Cd is linked to severe health

complications, including renal dysfunction, cardiovascular diseases, and reproductive disorders [1]. Therefore, mitigating Cd accumulation in food crops is an essential step toward reducing human health risks.

Conventional remediation strategies for Cd-contaminated agricultural soils (such as soil replacement, phytoextraction, and the application of chemical chelators) are often constrained by high costs, extended treatment periods, and the risk of secondary pollution, hindering their large-scale field application [2–4]. Consequently, in-situ immobilization has emerged as a highly practical alternative. This approach alters the chemical speciation of soil Cd, converting it from a highly bioavailable fraction to a stable, inactive form, thereby reducing its plant uptake and biological toxicity [5]. Biochar, a carbon-rich amendment produced via biomass pyrolysis under oxygen-limited conditions, has demonstrated exceptional potential in this regard [6]. Its extensive specific surface area, porous structure, and abundant oxygen-containing surface functional groups make it an ideal soil amendment [7–9]. Upon soil application, biochar effectively immobilizes Cd through multiple mechanisms, including surface adsorption, complexation, ion exchange, and precipitation, often facilitated by an increase in soil pH [10–13]. These synergistic processes fundamentally alter the existing forms of Cd in the soil, thereby significantly reducing its migration capacity and bioavailability to crops [14].

While the efficacy of biochar in remediating Cd-contaminated soils is well-documented, its application in cultivating leafy vegetables demands particular attention due to their naturally high transpiration rates and substantial heavy metal accumulation capacities. Recent investigations have increasingly focused on the biochar-leafy vegetable-Cd nexus. For instance, the application of various biochars has been shown to effectively reduce bioavailable Cd fractions in soil, thereby significantly lowering the BCF in commonly consumed leafy greens such as lettuce and Chinese cabbage [15,16]. Similarly, crop residue-derived biochar not only immobilized extractable Cd but also enhanced the biomass yield of spinach [17]. Beyond merely limiting root uptake, recent advances highlight that biochar amendments can systematically alleviate Cd-induced phytotoxicity, preserving chloroplast integrity and restoring photosynthetic capacity in leafy crops like pak choi [18]. Among leafy vegetables, amaranth is a globally important crop renowned for both its nutritional value and its strong tendency to accumulate Cd [19,20]. A recent study by Roy et al. [21] demonstrated that biochar could effectively mitigate the severe physiological and growth inhibitions caused by Cd pollution in red amaranth. Despite these promising findings, previous research has largely treated leafy vegetables as uniform biological models. The precise, cultivar-specific responses (e.g., green versus red amaranth cultivars) to varying doses of biochar under Cd stress, particularly, the potential trade-offs between Cd immobilization and plant growth disruption, remain insufficiently explored.

Tobacco straw is a massive agricultural residue in Southern China (especially Hunan), and its improper disposal (e.g., open burning) causes environmental issues. Converting it into biochar for remediation aligns with circular economy principles. Red and green amaranth are the two most widely consumed morphotypes globally. They inherently possess distinct secondary metabolite profiles (particularly anthocyanin accumulation in the red cultivar) and root development traits. These physiological differences make them ideal biological models to study genotypic variations in heavy metal tolerance and biochar responsiveness. The present study utilizes tobacco straw-derived biochar in a pot experiment to evaluate the effects of varying application rates on the growth, Cd uptake, and accumulation characteristics of two widely consumed amaranth varieties. We hypothesized that (1) tobacco straw biochar would effectively immobilize soil Cd and improve soil quality, and (2) red and green amaranth cultivars would exhibit distinct growth and physiological responses due to their inherent biochemical and genetic differences. The

ultimate objective is to determine optimal biochar application strategies that maximize crop yield while minimizing Cd accumulation, thereby providing a scientific basis and technical reference for the safe cultivation of leafy vegetables in Cd-contaminated agricultural lands. Therefore, the novelty of this study lies in elucidating the divergent, cultivar-specific responses of two *Amaranthus tricolor* cultivars to identical biochar treatments.

2. Materials and Methods

2.1. Preparation of Biochar and Soil Samples

Tobacco straw collected was naturally air-dried to a constant weight. The straw was cut into 10 cm lengths to fit the dimensions of the muffle furnace reactor chamber, ensuring uniform heat distribution without the need for energy-intensive pulverization before pyrolysis. The tobacco straw was pyrolyzed in a muffle furnace under a continuous nitrogen (N_2, 500 mL/min) gas flow. The N_2 atmosphere was utilized to maintain a strictly anoxic environment, which prevents the combustion (complete oxidation) of the biomass and promotes thermal carbonization, leading to the formation of a stable aromatic carbon skeleton. The muffle furnace heat at a heating rate of 10 °C·min^{-1} from room temperature to 360 °C, and maintained at this temperature for 2 h. The resulting biochar yield was approximately 35.0% and collected after cooling to room temperature. Soil samples (0–20 cm depth) were collected via a five-point sampling method from agricultural land historically affected by atmospheric deposition from a nearby industrial zone. This field had cadmium (Cd) contamination, resulting in poor agricultural productivity. Based on the regional soil survey data, the experimental soil is characterized as having a predominantly silty clay texture. After natural air-drying, the soil was ground and passed through a 2-mm sieve. The physicochemical properties and heavy metal contents of the initial soil and biochar are detailed in Table 1. The total Cd concentration of the soil was 2.18 mg/kg, which significantly exceeds the risk screening value for agricultural land according to the Chinese Soil Environmental Quality Standard (GB 15618-2018) [22]. The total Cd concentration of biochar was 1.04 mg/kg, which is well below the strict safety limits for biochar application.

Table 1. Basic information of test soil (initial unplanted soil) and biochar.

Material	pH	Organic Matter g/kg	Alkali-Hydro Nitrogen mg/kg	Effective P mg/kg	Available K mg/kg	Total Cd mg/kg	Effective Cd mg/kg
Soil	6.58	37.03	206.08	69.79	408.00	2.18	1.44
Biochar	9.40	Data unavailable	519.00	1.02	60,648.67	1.04	\

Note: The total organic carbon content of the biochar was not reliably determined because the Walkley-Black method is unsuitable for biochar matrices; therefore, this parameter is excluded from the characterization.

2.2. Characterization of Biochar

The surface functional groups of the biochar were identified using Fourier Transform Infrared (FTIR) spectroscopy within a wavenumber range of 400 to 4000 cm^{-1}. Biochar was ground to pass a 0.25-mm sieve, mixed with spectroscopy-grade KBr at a ratio of 1:50, and pressed into a transparent pellet. Spectra were acquired by averaging 100 scans at a resolution of 4 cm^{-1}, with a pure KBr pellet serving as the background.

The surface morphology and elemental distribution of the biochar were characterized using Scanning Electron Microscopy coupled with Energy Dispersive Spectroscopy (SEM-EDS). A trace amount of biochar powder was ultrasonically dispersed in deionized water. A drop of the suspension was placed on a clean silicon wafer, air-dried, and sputter-coated. The samples were observed using a field-emission scanning electron microscope (TESCAN MIRA LMS, Brno, Czech Republic) at an accelerating voltage of 15 kV under vacuum conditions.

To evaluate Cd adsorption, exactly 0.100 g of biochar was added to a centrifuge tube containing 25 mL of a 50 mg/L Cd solution. The initial pH of the Cd solution was adjusted to 5.0 using 0.1 M HNO_3 or NaOH to prevent metal precipitation. The mixture was agitated on a reciprocal shaker at 180 rpm and 25 °C for 24 h. Following centrifugation, the biochar pellet was collected, dried at 40 °C to a constant weight, and subsequently subjected to FTIR and SEM-EDS analyses to observe post-adsorption changes. The supernatant after centrifugation was collected to detect the Cd concentration.

2.3. Pot Experiment Design

A pot experiment was conducted in a greenhouse at the Hunan Vegetable Research Institute (Changsha, Hunan, China). Approximately 500 g of the prepared soil was weighed into plastic pots (20 cm diameter, 15 cm depth). This specific soil mass was selected as a standard for 30-day short-term seedling screening to ensure homogeneous root-biochar contact. Biochar was uniformly incorporated into the soil at weight ratios of 1% (5 g), 2% (10 g), and 5% (25 g), and no-biochar treatment as the control (hereafter referred to as CK). The amended soils were then irrigated to 75% of field capacity using deionized water and allowed to equilibrate. To ensure consistent baseline nutrition and eliminate nutrient deficiency as a confounding variable, a uniform basal fertilization was applied to all pots prior to planting. Specifically, 1.0 g of a water-soluble compound fertilizer (N-P_2O_5-K_2O=15-15-15, Cd concentration below detection limit) was completely dissolved in deionized water and evenly irrigated into each pot (containing 500 g of soil). This application supplied precisely 150 mg of N, 65.4 mg of P, and 124.5 mg of K per pot.

Two common amaranth cultivars, 'Yuanyanghong' (a red variety) and 'Dayeqing' (a green variety), were used in this study: Seeds were obtained from a local agricultural market in Changsha, China. The experiment was conducted in a greenhouse with a day/night temperature of approximately 25/20 °C and 60–70% relative humidity. Seeds were sown in excess and thinned to exactly 5 plants per pot upon emergence. Soil moisture was maintained at 75% of field capacity by weighing the pots every two days and replenishing the lost water with deionized water. Each combination of cultivar and biochar treatment consisted of five biological replicates. Plants were harvested 30 days after sowing.

2.4. Determination of Pn, Fv/Fm, and SPAD Value

The net photosynthetic rate (Pn) of the fourth fully expanded leaf of the amaranth plants was measured using a portable photosynthesis system (LI-6800, LI-COR Biosciences, Lincoln, NE, USA) between 10:00 and 12:00 on a clear day. The leaf chamber temperature and relative humidity were maintained at 28 °C and 50%, respectively, with a photosynthetic photon flux density of 600 $\mu mol \cdot m^{-2} \cdot s^{-1}$. Data were recorded after an equilibration period of approximately 10 min.

At 20 days post-sowing, the maximal photochemical efficiency of PSII (Fv/Fm) and relative chlorophyll content (SPAD values) were assessed on leaves at the same physiological position. Fv/Fm was measured using a chlorophyll fluorescence analyzer (FluorPen FP 110, Photon Systems Instruments, Drásov, Czech Republic), and SPAD values were determined using a handheld chlorophyll meter (SPAD-502 Plus, Konica Minolta, Tokyo, Japan). Measurements were taken in triplicate on the same leaf to obtain an average value, with three leaves assessed per plant across five plants per treatment.

2.5. Sample Collection and Pre-Treatment

To ensure statistical rigor, the pot was treated as the experimental unit. At harvest, all 5 plants within each replicate pot were measured for plant height and stem diameter, and the values were averaged to represent that specific pot. Subsequently, 3 independent pots (n = 3) from each treatment were randomly selected for destructive sampling. The

plants from these pots were thoroughly rinsed with tap water, followed by three rinses with deionized water to eliminate any surface adhering soil or Cd contamination. Then the plants were divided into shoots and roots to record fresh weight (FW), then dried at 65 °C to a constant weight (DW), and stored for Cd concentration analysis. Concurrently, fresh leaves from the remaining replicate pots were collected, frozen in liquid nitrogen, and stored at −80 °C for biochemical assays. During harvest, rhizosphere soil was carefully collected. Plants were uprooted, and loosely bound soil was shaken off. The soil strongly adhering to the roots (approx. 1–2 mm thick) was gently collected using a sterile brush. The rhizosphere soil from the 3 sampled pots per treatment was combined, air-dried, and sieved for analysis.

2.6. Determination of Cd Accumulation and Quality Indicator in Amaranth

Cd concentrations in plant tissues were determined according to the Chinese National Standard (GB 5009.268-2016) [23]. Briefly, 0.5 g of the ground dried shoot and root samples (from Section 2.5) were accurately weighed and digested in triplicate with high-purity nitric acid (HNO_3) using a closed-vessel microwave digestion system. The digested solutions were diluted to a constant volume and analyzed using a graphite furnace atomic absorption spectrometer (GFAAS, PinAAcle 900T, PerkinElmer, Waltham, MA, USA) equipped with an electrodeless lamp (EDL) operating at a wavelength of 228.8 nm. The furnace temperature program was optimized for drying, ashing, and atomization. To optimize measurement and minimize matrix interference, 5 µL of 1% (*w*/*v*) ammonium dihydrogen phosphate was employed as a matrix modifier. An external standard method was used for quantification, yielding a highly linear calibration curve (R > 0.995). Procedural blanks and certified plant reference materials were included in each batch to ensure analytical accuracy and precision. The contents of total anthocyanin (determined via the pH differential method), Ascorbic acid (AsA, determined via titration), total soluble protein (Coomassie brilliant blue G-250 method), and amino acid (AA, ninhydrin colorimetry) were determined according to the instructions of reagent kit (Shanghai Zhuocai Biological Co., Ltd., Shanghai, China).

2.7. Analysis of Total Cd and Its Chemical Speciation in Soil

Soil pH and Soil electrical conductivity (EC) were measured using a pH meter (PHS-3E, Leici, Shanghai, China) and conductivity meter (DDS-307A, Leici, Shanghai, China) in a 1:2.5 (*w*/*v*) soil-to-deionized water suspension. Total soil Cd concentration was determined following the standard method HJ 1315-2023 [24]. Air-dried soil samples (passed through a 100-mesh sieve) were completely digested using an HNO_3-HF-H_2O_2 mixture in a microwave digestion system. The digests were analyzed using Inductively Coupled Plasma Mass Spectrometry (ICP-MS, NexION 2000, PerkinElmer, USA). Internal standards (^{103}Rh) were spiked online to correct for matrix effects. Instrument drift was strictly monitored, and sample analysis was accepted only when internal standard recoveries remained within 90–110%.

The chemical speciation of soil Cd was fractionated using a modified sequential extraction procedure based on GB/T 25282-2010 [25]. The fractions were operationally defined as follows: (1) Exchangeable fraction: Soil was extracted with 1 mol/L $MgCl_2$ (pH 7.0) via shaking at 25 °C for 2 h; (2) Reducible (Iron-manganese oxide-bound) fraction: The residue from step 1 was extracted with 0.04 mol/L hydroxylamine hydrochloride in 25% (*v*/*v*) acetic acid via shaking at 96 °C for 4 h; (3) Residual fraction: The final residue was completely digested using the microwave digestion method described above. The Cd concentrations in the extraction solutions were determined using Inductively Coupled Plasma Optical Emission Spectrometry (ICP-OES, Optima 8300, PerkinElmer, USA).

Strict QA/QC procedures were implemented for all Cd determinations. External standard calibration curves exhibited excellent linearity ($R^2 > 0.999$). The limits of detection (LOD) and limits of quantification (LOQ) for Cd were 0.03 mg/kg and 0.12 mg/kg, respectively. Procedural blanks (reagent blanks) were included in every analytical batch (n = 3), and all sample results were blank-corrected. Analytical accuracy and precision were validated using Certified Reference Materials (CRMs) for soil (RMU189), certified Cd: (0.628 ± 0.061 mg/kg). The recovery rates for the CRMs ranged from 92% to 105%, and the relative standard deviation (RSD) of analytical replicates was consistently <5%.

2.8. Statistical Analysis

For growth parameters, five biological replicates (n = 5) were measured to account for individual plant phenotypic variance. For subsequent destructive biochemical and soil analyses, samples from the replicates were pooled to create three independent composite samples (n = 3) per treatment, which is a standard practice to reduce analytical variability while maintaining statistical validity. All data are presented as the mean ± standard error (SE) of the biological replicates. Statistical analyses were performed using SPSS 20.0. A two-way analysis of variance was conducted to evaluate the main effects of biochar, cultivar, and their interactive effects (Biochar × Cultivar) on Cd accumulation and plant growth. Significant differences among treatment means were determined using Tukey's test at $p < 0.05$. Data normality and homogeneity of variances were verified using the Shapiro-Wilk and Levene's tests, respectively, prior to conducting the two-way ANOVA.

3. Results

3.1. Characteristics of the Prepared Biochar

The Cd adsorption experiment revealed that the tobacco straw-derived biochar exhibited a remarkable removal capacity for Cd in aqueous solutions. Specifically, the Cd concentration in the biochar-treated solution was significantly reduced by 98.7% compared to the control group (Figure 1A), confirming the biochar as a highly efficient Cd adsorbent. SEM analysis indicated that the pristine biochar possessed a rough surface with an abundant pore structure and well-defined channels (Figure 1B). EDS revealed that the pristine biochar was predominantly composed of C (54.1%) and O (17.5%), along with minor mineral elements (Na, Mg, P, K, Ca, and Fe), whereas its initial Cd content was negligible (0.1%). In contrast, following Cd adsorption, numerous aggregates and flocculent structures were observed depositing on the surface and within the pores of the biochar, partially blocking the channels (Figure 1C). Correspondingly, the EDS spectra of the post-adsorption biochar displayed distinct characteristic peaks for Cd, with its mass fraction increasing to 1.5%, accompanied by a relative decrease in the proportions of Ca, Mg, and Fe.

FTIR was employed to elucidate the role of surface oxygen-containing functional groups in Cd adsorption. The spectra demonstrated that the characteristic infrared peaks of the biochar underwent notable shifts following Cd adsorption (Figure 1D,E). Specifically, the absorption peak assigned to C=C/C=O shifted from 1608 cm^{-1} to 1617 cm^{-1}, and the -CH_2 bending vibration shifted from 1411 cm^{-1} to 1418 cm^{-1}. Most notably, the absorption peak corresponding to the C-O stretching vibration exhibited a pronounced shift from 1111 cm^{-1} to 1091 cm^{-1}, indicating the strong involvement of these functional groups in Cd complexation.

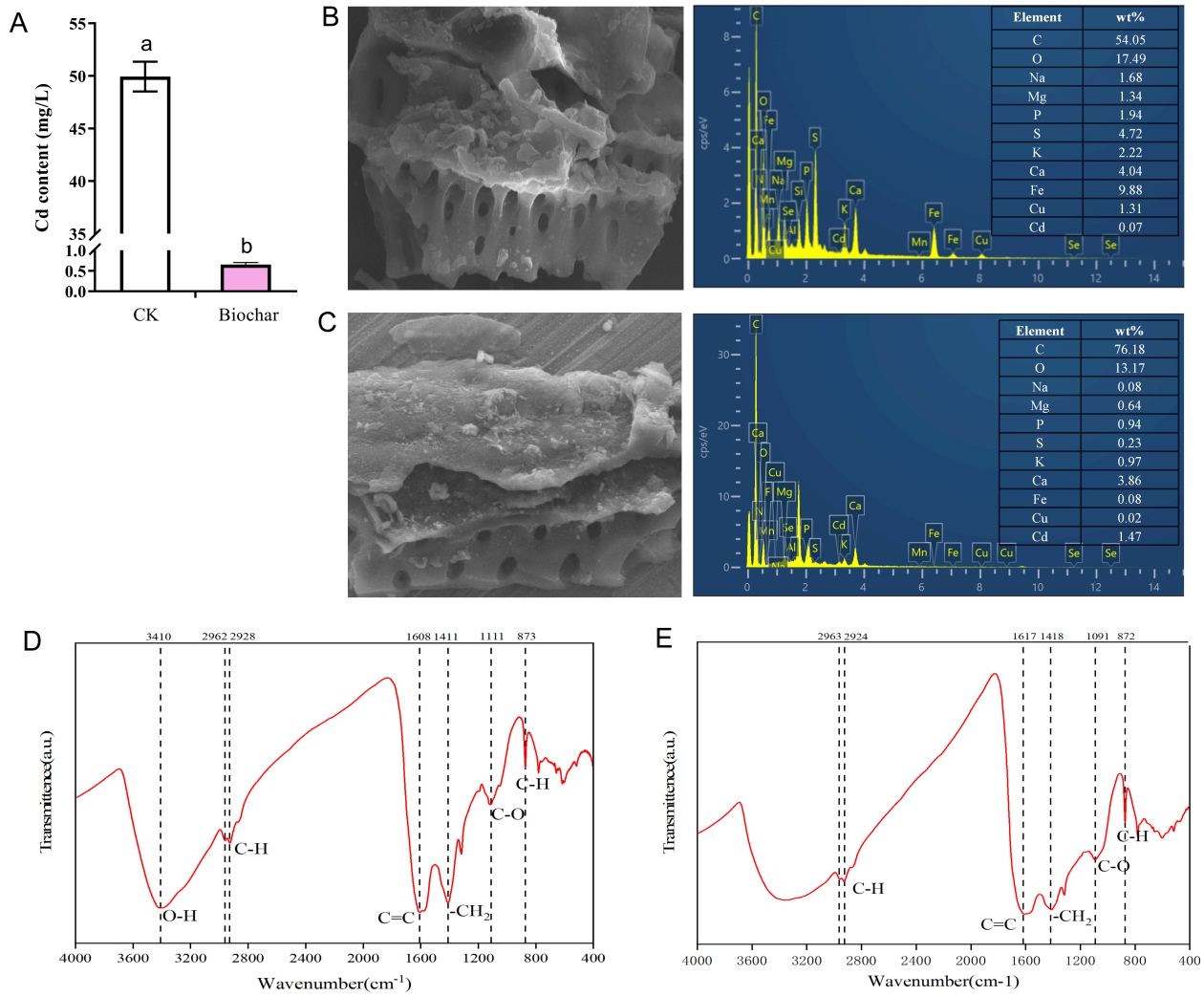

Figure 1. Characterization of biochar before and after Cd adsorption. (**A**) The Cd concentration in the aqueous solution after using biochar for Cd adsorption. (**B**,**C**) The SEM and EDS of untreated biochar (**B**) and biochar after Cd adsorption (**C**). (**D**,**E**) The FTIR of untreated biochar (**D**) and biochar after Cd adsorption (**E**). The letters in (**A**) represent the significant difference of the treatments ($p < 0.05$). CK means no-biochar treatment. The peak in (**B**,**C**) indicates the presence of the specific element. The valley in (**D**,**E**) represents the presence of specific functional groups.

3.2. Effects of Biochar on Soil pH and Cd Fractions

Two-way ANOVA indicated that soil pH was significantly influenced by the main effect of biochar ($p < 0.01$), while the cultivar type and their interaction were not significant (Figure 2A). In soil cultivated with red amaranth, the pH increased gradually with ascending biochar application rates. A similar mild upward trend was observed in the green amaranth soil, confirming that the pH-buffering effect of biochar acts independently of the amaranth variety. The application of biochar induced highly divergent, cultivar-specific alterations in soil EC (Figure 2B). A significant interaction was shown between cultivar and biochar treatments (C × B, $p < 0.05$). For the red cultivar, soil EC value decreased with the increase in biochar application concentration, dropping 59.6% under the 5% biochar treatment compared with CK. Conversely, for the green cultivar, biochar application led to a higher EC value, which surged 1.77 times higher under 5% biochar treatment than that of CK.

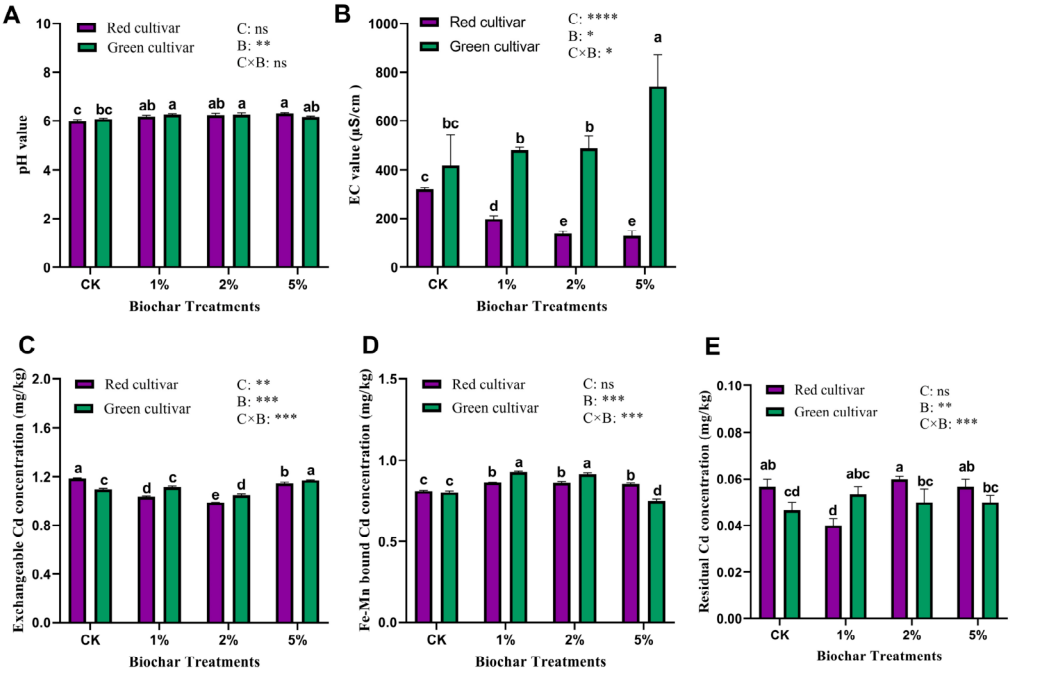

Figure 2. Effects of different biochar treatments on soil pH (**A**), soil EC (**B**), soil exchangeable Cd concentration (**C**), Fe-Mn bound Cd concentration (**D**), and residual Cd concentration (**E**) in red and green amaranth cultivars. Data are presented as mean ± standard error (n = 3). Different lowercase letters indicate significant differences among all treatment combinations according to Tukey's test at $p < 0.05$. The insert text indicates the main and interactive effects based on a two-way ANOVA (C: Cultivar, B: Biochar, C × B: Cultivar × Biochar, * $p < 0.01$, ** $p < 0.01$, *** $p < 0.001$, **** $p < 0.0001$, ns: not significant).

The three operationally defined chemical forms of soil Cd responded to the biochar application with highly significant interactive effects (C × B, $p < 0.001$) (Figure 2C–E). Overall, biochar addition effectively reduced the exchangeable Cd fraction in the red amaranth soil. Compared to CK, the exchangeable Cd concentration was significantly reduced by 12.9% and 17.0% under the 1% and 2% treatments, respectively, though this reduction attenuated to 3.6% at the 5% dose. Concurrently, the Fe-Mn bound Cd fraction significantly increased by 7.1%, 6.4%, and 5.6% across the respective treatments. The residual Cd concentration in red amaranth soil significantly decreased by 32.7% under the 1% treatment but remained comparable to CK under the 2% and 5% treatments. Interestingly, the transformation of Cd fractions in the green amaranth cultivated soil exhibited a markedly different and somewhat paradoxical pattern. While the 2% biochar treatment significantly decreased the exchangeable Cd by 4.5%, the highest dose (5%) induced a significant increase of 6.7% relative to CK (Figure 2C). This anomaly was mirrored in the Fe-Mn bound Cd fraction (Figure 2D), which significantly increased under the 1% and 2% treatments but plummeted strictly below the control level at the 5% dose. The residual Cd concentration in the green cultivar soil was generally unaffected by the higher doses, though a significant transient increase was observed at the 1% application rate (Figure 2E).

3.3. Effects of Biochar on Amaranth Plant Growth

The application of biochar significantly influenced the growth parameters of amaranth, with a highly significant interaction observed between cultivar and biochar treatments (C × B, $p < 0.001$), particularly for shoot biomass (Table 2). For the red cultivar, biochar exerted a distinctly stimulatory effect on vegetative growth. Plant height, shoot fresh weight (FW), and shoot dry weight (DW) all reached their maximums under the 2% biochar treatment, exhibiting significant increases of 27.3%, 67.2%, and 58.6%, respectively,

compared to the CK. Additionally, stem width was significantly enhanced by 25.3% under the 5% biochar treatment. Notably, while shoot biomass was significantly promoted, root parameters (Root FW and DW) remained statistically unaffected by biochar application. In contrast, the green cultivar exhibited a strikingly different, and occasionally inhibitive, growth response. Plant height and stem width, showed no significant differences from the CK across all biochar doses. However, 2% biochar treatment significantly decreased shoot FW and DW by 24.0% and 28.9%, respectively. Under the 5% treatment, while shoot FW recovered and showed no significant difference from the CK, shoot DW and root DW were significantly reduced.

Table 2. Effects of biochar application on the growth parameters of two amaranth cultivars.

Cultivar	Biochar Treatment	Plant Height (cm)	Stem Width (mm)	Shoot FW (g)	Shoot DW (g)	Root FW (g)	Root DW (g)
Red amaranth	CK	7.29 ± 0.21 d	4.46 ± 0.14 b	6.53 ± 0.58 e	0.70 ± 0.09 e	1.20 ± 0.29 b	0.11 ± 0.03 c
	1%	8.78 ± 0.76 c	4.74 ± 0.41 ab	9.15 ± 0.85 d	0.96 ± 0.02 d	1.45 ± 0.16 ab	0.13 ± 0.02 c
	2%	9.28 ± 0.12 bc	5.50 ± 0.17 a	10.85 ± 0.42 c	1.11 ± 0.05 d	1.35 ± 0.12 b	0.13 ± 0.02 c
	5%	8.74 ± 0.59 c	5.65 ± 0.40 a	8.19 ± 0.65 d	0.90 ± 0.04 de	1.29 ± 0.13 b	0.12 ± 0.02 c
Green amaranth	CK	9.86 ± 0.46 abc	5.40 ± 0.04 ab	15.03 ± 0.09 a	1.94 ± 0.03 a	1.94 ± 0.17 a	0.27 ± 0.03 ab
	1%	11.00 ± 0.35 a	5.29 ± 0.42 ab	12.94 ± 0.26 b	1.72 ± 0.10 ab	1.91 ± 0.16 a	0.29 ± 0.05 a
	2%	10.51 ± 0.46 ab	5.10 ± 0.24 ab	11.43 ± 0.26 c	1.38 ± 0.04 c	1.43 ± 0.15 ab	0.19 ± 0.01 bc
	5%	9.98 ± 0.46 abc	4.70 ± 0.15 ab	15.84 ± 0.78 a	1.62 ± 0.13 b	1.51 ± 0.03 ab	0.15 ± 0.02 c
Two-way ANOVA							
Cultivar (C)		***	ns	***	***	**	***
Biochar (B)		*	ns	ns	ns	ns	ns
C × B		ns	*	***	***	ns	ns

Note: FW represents Fresh Weight; DW represents Dry Weight. Different lowercase letters indicate significant differences among all treatment combinations according to Tukey's test at $p < 0.05$. The main and interactive effects based on the two-way ANOVA: * $p < 0.05$, ** $p < 0.01$, *** $p < 0.001$, ns: not significant.

3.4. Effects of Biochar on Cd Accumulation in Amaranth

Two-way ANOVA revealed that Cultivar, Biochar, and their interaction (C × B) all had highly significant effects ($p < 0.001$) on Cd accumulation in both roots and shoots (Figure 3A,B). While biochar treatments significantly reduced Cd accumulation in both cultivars, the inhibitory effects were highly cultivar-dependent. Root Cd concentration in red amaranth decreased progressively with increasing biochar rates, showing drastic reductions of 42.8%, 47.5%, and 51.5% under the 1%, 2%, and 5% treatments, respectively, compared to CK. Although a similar decreasing trend was observed in green amaranth roots, the magnitude of reduction was much smaller (20.3%, 28.1%, and 30.9%, respectively), with no significant difference noted between the 2% and 5% doses. Consistent with root data, shoot Cd concentrations were also significantly mitigated, but biochar exerted a much more pronounced inhibitory effect on the red cultivar. Relative to CK, shoot Cd in red amaranth was substantially reduced by 18.5%, 37.6%, and 25.8% under the 1%, 2%, and 5% treatments, respectively. In sharp contrast, the corresponding reductions in green amaranth were only 11.8%, 4.6%, and 4.6%. To evaluate the practical implications for food safety, the shoot Cd concentrations were converted from a DW to a FW basis using the respective DW/FW ratios (Table 2). Under 2% biochar treatment, the estimated FW Cd concentration in the red cultivar was reduced to 0.20 mg/kg, effectively meeting the stringent regulatory safety threshold. In contrast, while biochar treatments significantly

reduced Cd accumulation in the green cultivar, the final concentrations (0.33–0.40 mg/kg FW) remained above the safe limit.

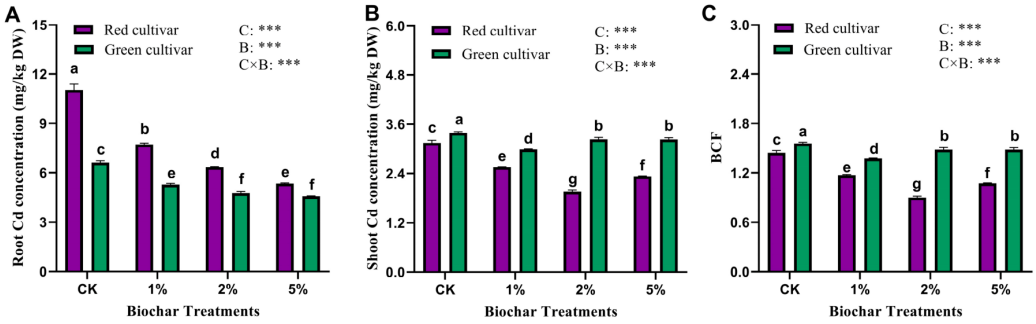

Figure 3. Effects of different biochar treatments on Root Cd concentration (**A**), Shoot Cd concentration (**B**), and Bioconcentration Factor (BCF) (**C**) in red and green amaranth cultivars. Data are presented as mean ± standard error (n = 3). Different lowercase letters indicate significant differences among all treatment combinations according to Tukey's test at $p < 0.05$. The insert text indicates the main and interactive effects based on a two-way ANOVA (C: Cultivar, B: Biochar, C × B: Cultivar × Biochar, *** $p < 0.001$).

The bioconcentration factor (BCF) was calculated to assess the plants' capacity to accumulate Cd from the soil (Figure 3C). The highly significant interaction ($p < 0.001$) indicated distinct Cd uptake strategies between the two varieties under biochar amendment. For red amaranth, the 2% biochar treatment yielded the lowest BCF (a 37.8% reduction vs. CK), followed by the 5% (25.8%) and 1% (18.5%) treatments. Conversely, for green amaranth, the maximum reduction in BCF prematurely occurred under the 1% treatment (11.8%), with the 2% and 5% treatments showing significant but much smaller reductions (4.6% and 4.6%, respectively, with no significant difference between the two higher doses).

3.5. Effects of Biochar on Photosynthetic and Fluorescence Parameters

Biochar application exhibited cultivar-specific effects on the Pn of amaranth (Figure 4A). For the red cultivar, the 1% biochar treatment significantly enhanced Pn by 55.52% compared to CK. However, this stimulatory effect diminished at higher application rates, with the 2% and 5% treatments showing non-significant increases. Conversely, for the green cultivar, biochar application did not significantly alter Pn, although slight numerical fluctuations were observed, including a non-significant decrease of 5.6% at 1%, and marginal increases of 31.3% and 28.7% under the 2% and 5% treatments, respectively.

SPAD values differed significantly between the two cultivars but were unaffected by biochar treatments (Figure 4B). In both the red and green cultivars, biochar application resulted in no statistically significant changes relative to their respective CKs across all doses. While minor numerical variations were noted, such as subtle increases of 12.9%, 8.3%, and 5.9% in the green cultivar under the 1%, 2%, and 5% treatments, respectively, the two-way ANOVA confirmed that the biochar main effect was not significant. Furthermore, the maximum photochemical efficiency of PSII (Fv/Fm) demonstrated a significant interaction between cultivar and biochar treatments (Figure 4C). While the Fv/Fm of the green cultivar remained stable with no significant differences compared to its control, the red cultivar exhibited a declining trend at higher biochar doses, culminating in a significant reduction under the 5% treatment compared to the CK.

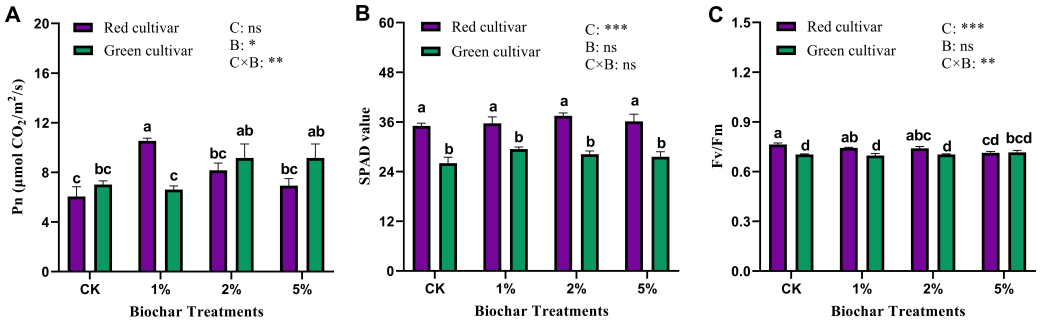

Figure 4. Effects of different biochar treatments on Net photosynthetic rate (Pn) (**A**), SPAD value (**B**), and The maximum quantum efficiency of PSII (Fv/Fm) (**C**) in red and green amaranth cultivars. Data are presented as mean ± standard error (n = 3). Different lowercase letters indicate significant differences among all treatment combinations according to Tukey's test at $p < 0.05$. The insert text indicates the main and interactive effects based on a two-way ANOVA (C: Cultivar, B: Biochar, C × B: Cultivar × Biochar, * $p < 0.05$, ** $p < 0.01$, *** $p < 0.001$, ns: not significant).

3.6. Effects of Biochar on the Antioxidant and Nutritional Profiles of the Amaranth

Biochar application induced variable, cultivar-specific effects on the antioxidant and nutritional profiles of the amaranth (Figure 5). Regarding antioxidants, the total anthocyanin content in the red cultivar was significantly reduced by 27.8%, 25.7%, and 41.0% under the 1%, 2%, and 5% treatments, respectively, compared to CK. In contrast, the green cultivar maintained consistently lower anthocyanin levels that remained unaffected by biochar application (Figure 5A). Furthermore, biochar had no statistically significant effect on the AsA content for either cultivar (Figure 5B). Although a slight numerical peak was observed in the red amaranth under the 1% treatment (a 20.4% increase relative to CK), the two-way ANOVA confirmed no significant main effects or interactions for AsA.

In terms of nutritional quality, soluble protein and amino acid contents exhibited distinct response patterns. For soluble protein, while biochar applied at 1%, 2%, and 5% numerically increased the content in red amaranth by 21.6%, 32.7%, and 16.7%, respectively, these changes were not statistically significant compared to the CK (Figure 5C). However, in green amaranth, the 2% biochar treatment significantly elevated soluble protein content, whereas the 1% and 5% doses resulted in non-significant numerical increases (18.7% and 17.9%, respectively). The 1% treatment significantly elevated total amino acid content in both red and green cultivars, yielding an impressive numerical increase of 42.3% in the green variety (Figure 5D). However, higher biochar doses negated this benefit: in green amaranth, amino acid content under the 2% and 5% treatments returned to levels statistically comparable to the CK. More notably, in the red cultivar, while the 2% treatment showed no significant difference from the CK, the 5% application rate led to a significant reduction in total amino acid content.

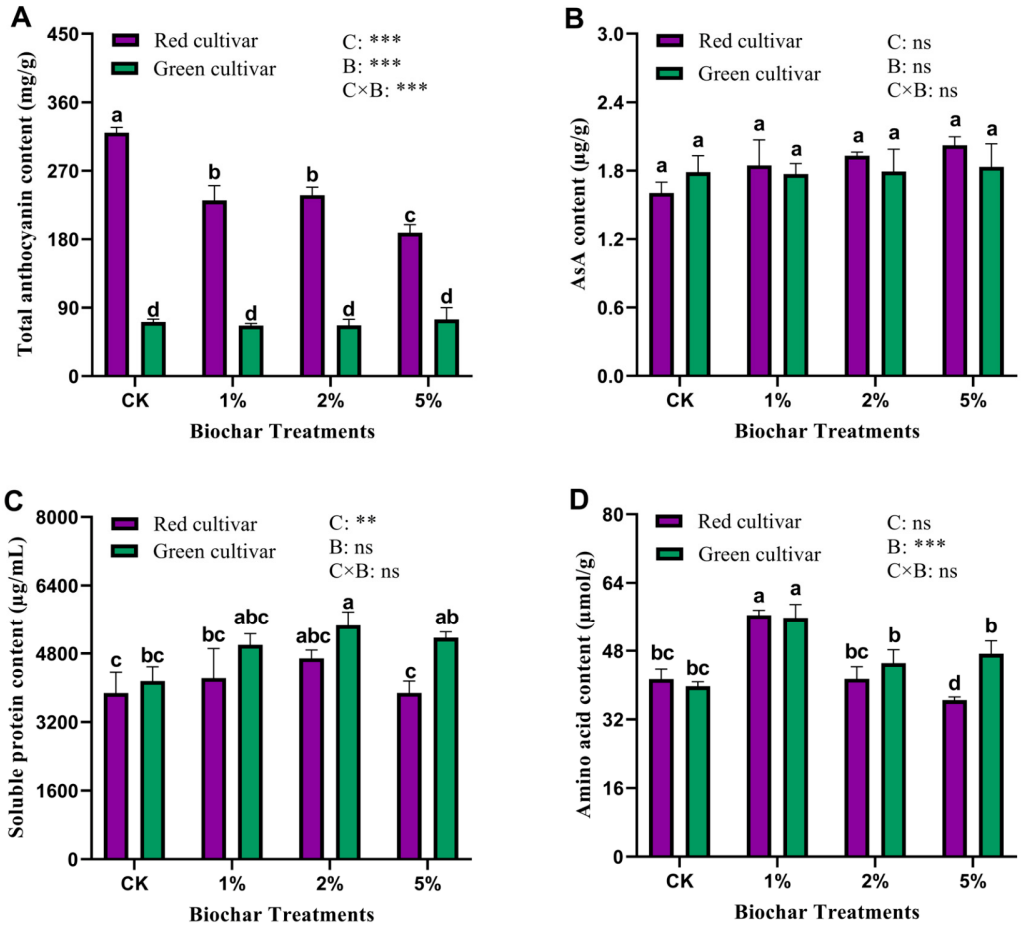

Figure 5. Effects of different biochar treatments on the content of total anthocyanin (**A**), ascorbic acid (AsA) (**B**), soluble protein (**C**), and amino acid (**D**) in red and green amaranth cultivars. Data are presented as mean ± standard error (n = 3). Different lowercase letters indicate significant differences among all treatment combinations according to Tukey's test at $p < 0.05$. The insert text indicates the main and interactive effects based on a two-way ANOVA (C: Cultivar, B: Biochar, C × B: Cultivar × Biochar, ** $p < 0.01$, *** $p < 0.001$, ns: not significant).

3.7. Correlation Analysis

Pearson correlation analysis was conducted to elucidate the relationships among 20 measured parameters for both cultivars (Figure 6). In red amaranth, shoot Cd, root Cd concentration, and BCF exhibited significant positive correlations with soil exchangeable Cd, Fv/Fm, and total anthoyanin content, but were significantly negatively correlated with soil pH, EC value, Fe-Mn oxide-bound Cd, plant height, stem diameter, shoot FW, and shoot DW (Figure 6A). Soil exchangeable Cd was negatively correlated with plant growth metrics (plant height, FW, DW) and Pn. The correlations for Fe-Mn oxide-bound Cd were inversely related to those of exchangeable Cd.

In contrast, the correlations among parameters in green amaranth were generally weaker (Figure 6B). Shoot Cd and BCF values were significantly negatively correlated with residual Cd, Fe-Mn oxide-bound Cd, and AA content. Furthermore, soil exchangeable Cd was significantly negatively correlated with Fe-Mn oxide-bound Cd but showed a significant positive correlation with shoot FW. Residual Cd concentration exhibited a significant positive correlation with soil pH and AA content.

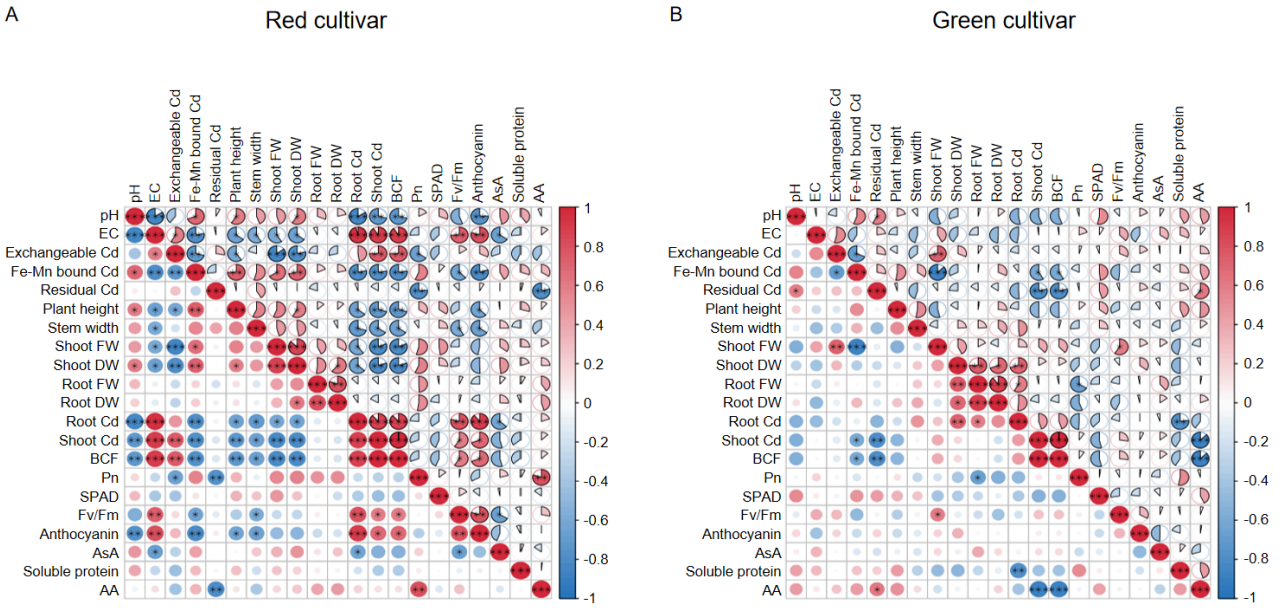

Figure 6. Correlation analysis among various indicators of the red and green amaranth. (**A**,**B**) The correlation analysis of the indicators measured of red (**A**) and green (**B**) amaranth. The asterisks represent the significant difference of different treatments ($p < 0.05$), * $p < 0.05$, ** $p < 0.01$, *** $p < 0.001$. Red color represents positive correlation, blue color represents negative correlation. The dot size and sector are synchronized with the significance.

4. Discussion

4.1. Mechanisms of Cadmium Immobilization by Biochar: From Porous Structure to Soil Amelioration

The findings of this study demonstrate that tobacco straw-derived biochar effectively reduces the bioavailability of Cd in soil (Figure 2). This efficacy is attributed to both the inherent physicochemical properties of the biochar and its ameliorative effects on the soil microenvironment. First, the specific physicochemical characteristics of biochar form the foundation of its remediating function [26]. Scanning electron microscopy (SEM) analysis revealed that the pristine biochar possessed an abundant porous structure (Figure 1B), that provides numerous physical sites for the adsorption of soil Cd^{2+} [27–29]. Following Cd exposure, the observation of aggregates and flocculent structures partially blocking the biochar channels (Figure 1C) suggests that Cd was immobilized via precipitation or surface complexation [30]. Energy-dispersive X-ray spectroscopy (EDS) results showed a distinct increase in Cd mass fraction accompanied by a relative decrease in mineral elements (Ca, Mg, Fe) on the post-adsorption biochar (Figure 1C). This elemental shift implies that the adsorption process involved significant ion exchange between the inherent biochar mineral cations and Cd^{2+} [31]. More importantly, Fourier-transform infrared spectroscopy (FTIR) confirmed the active participation of oxygen-containing functional groups (e.g., -OH, C-O) and π-electron systems (C=C), as evidenced by their peak shifts post-adsorption (Figure 1E). In this study, tobacco straw biochar was produced at a relatively low pyrolysis temperature of 360 °C to maximize the preservation of oxygen-containing functional groups (e.g., carboxyl and hydroxyl), which drive Cd immobilization primarily through surface complexation rather than physical pore-filling [32]. Although low-temperature biochar generally possesses a less developed physical pore structure [33], our aqueous sorption assays confirmed its inherent Cd-binding capacity. However, the lack of specific surface area (S_{BET}) data, a key parameter influencing physical sorption, limits a fully comprehensive interpretation of the physical mechanisms and their direct comparison with previous studies.

Secondly, the application of biochar profoundly altered key soil properties, which synergistically reinforced Cd immobilization [34]. We observed a biochar-induced elevation in soil pH, particularly in the red amaranth soil. An elevated pH enhances Cd immobilization by increasing the negative surface charge of soil colloids and biochar functional groups (enhancing electrostatic adsorption), while concurrently promoting the precipitation of Cd^{2+} with OH- or CO_3^{2-} to form less soluble compounds, such as $Cd(OH)_2$ and $CdCO_3$ [35,36]. Our soil speciation analysis provides direct evidence for this transformation: biochar treatments significantly decreased the highly bioavailable exchangeable Cd fraction while concurrently increasing the more stable Fe-Mn oxide-bound fraction (Figure 2D,E). This confirms that biochar not only directly captures Cd but also acts as an environmental driver, facilitating the transformation of Cd from labile to inert forms, thereby fundamentally reducing the risk of plant uptake. Interestingly, a slight decrease in the residual Cd fraction was observed in the red cultivar soil under the 1% treatment. This phenomenon might be attributed to minor initial shifts in soil equilibrium where low biochar doses temporarily mobilized certain stable fractions before bulk immobilization dominated at higher doses. Alternatively, it may reflect the inherent analytical variability often associated with sequential chemical extraction procedures (e.g., the BCR method).

Collectively, these chemical interactions, including electrostatic attraction, ion exchange, and surface complexation, enable the biochar to firmly sequester free Cd^{2+} onto its surface [37,38]. Although our preliminary aqueous adsorption assay confirmed the biochar's intrinsic Cd-binding capacity, it simplifies the competitive ion dynamics and organic matter interactions inherent in natural soils. Nevertheless, the successful reduction of exchangeable Cd and plant uptake in the subsequent pot experiments validates its practical efficacy in a real soil matrix. The lack of comprehensive physicochemical data (specifically S_{BET}) limits a holistic mechanistic interpretation. Future research should incorporate detailed biochar characterization and soil-biochar mixture assays to precisely decouple the chemical and physical mechanisms of heavy metal mitigation in complex agronomic systems.

4.2. Species-Specific Plant Responses: The Dual Effects of Biochar on Growth, Physiology, and Quality

A pivotal finding of this study is the marked species-specific response of the two amaranth cultivars to biochar application. While biochar uniformly reduced Cd accumulation, it exerted divergent effects on the growth, physiology, and nutritional quality of the red and green varieties. For red amaranth, biochar application yielded consistently synergistic outcomes. Specifically, the 2% application rate significantly promoted plant height and biomass (shoot FW and DW) (Table 2). Furthermore, it maintained photosynthetic rate (Pn) (Figure 4A) and nutritional quality indicators, including ascorbic acid and soluble protein (Figure 5B,C). This robust performance can be largely attributed to genotypic advantages. Previous studies have indicated that Amaranthus species exhibit significant intraspecific variation in environmental stress tolerance [39,40]. We supposed that red amaranth cultivars are inherently rich in betacyanins and anthocyanins, which confer a powerful antioxidant defense system capable of scavenging reactive oxygen species (ROS) induced by heavy metals or sudden environmental shifts [41,42]. This physiological buffer likely enabled red amaranth to rapidly acclimate to the biochar-amended soil, allowing it to fully utilize the improved soil physical structure and supplementary nutrients provided by the biochar [43,44]. The resulting biomass expansion consequently led to a "biodilution" effect, further lowering the tissue Cd concentration. However, since specific oxidative stress markers (e.g., ROS accumulation, lipid peroxidation) were not quantified in this study, this physiological mechanism requires further investigation.

Conversely, green amaranth exhibited an antagonistic growth response. Despite a reduction in Cd uptake, its biomass was notably inhibited under biochar treatments (Table 2). Lacking the intense, pigment-mediated antioxidant protection of the red cultivar, green amaranth may be hypersensitive to the physicochemical alterations induced by biochar. For instance, the biochar-induced elevation in soil pH or the strong adsorption capacity of the amendment might have immobilized essential micronutrients (e.g., Fe, Zn) alongside Cd, inducing localized nutrient deficiencies [45]. Additionally, biochar has the potential to adsorb low-molecular-weight organic acids secreted by plant roots, which could disrupt the specific nutrient acquisition strategies of green amaranth [46]. These findings highlight a distinct physiological trade-off in the green cultivar: although biochar successfully alleviated direct Cd toxicity (as evidenced by reduced tissue Cd), the potential side effects of the biochar, such as elevated soil pH tying up micronutrients or inducing localized osmotic stress, likely overpowered these benefits, resulting in net growth inhibition. This underscores the critical need for "crop-amendment matching" in soil remediation practices.

To contextualize our findings within the broader landscape of heavy metal remediation, we compared our results with recent worldwide studies utilizing pristine or modified biochar for Cd immobilization in leafy vegetables (Table 3). Previous studies have consistently demonstrated the efficacy of various biochars in reducing Cd availability and alleviating oxidative stress in crops such as spinach, lettuce, and Brassica species including pak choi [16,17,47,48]. Furthermore, advanced composites, such as nanoscale zero-valent iron (nZVI) supported on biochar, have proven highly effective in mitigating heavy metal uptake and restoring photosynthetic capacity in leafy greens [18,49]. However, this comparative analysis highlights a critical, often overlooked dimension addressed in our study: cultivar-specific sensitivity. While the red amaranth in our study conformed to the widely reported beneficial trends, the green amaranth exhibited significant growth inhibition at higher biochar doses. Therefore, our study prevents the overstatement of biochar's universal benefits, emphasizing instead that remediation strategies must be strictly tailored to specific crop cultivars to avoid unintended agronomic trade-offs.

Table 3. Comparison of the present study with literature on Cd immobilization and growth responses in leafy vegetables using pristine or modified biochar.

Crop	Soil Type	Biochar Feedsock (PyrolysisTemp.)	Dose (*w*/*w*)	Exp.Setup	Initial Soil Cd (mg/kg)	Cd Reduction in Edible Tissue	Growth Response/ Mechanisms	Ref.
pak-choi & lettuce	Cultivated soil contaminated Cd	Husk (Temperature not report)	4.4% for pak-choi; 2.1% for lettuce	Pot/Field	10~13	Reduced Cd accumulation by 16% for pak-choi and by 18% for lettuce	Significantly increase soil pH and reduce the bioavailability of Cd	[16]
Spinacia oleracea L.	Sandy loam	Pigeon pea straw (300 °C)	0.25%, 0.5%	Pot/Field	0.20	Reduced Cd accumulation by 12.16~34.5%	Reduce the mobility and plant availability of Cd	[17]
Pak choi	Sandy loam	Maize straw (500 °C)	1%, 3%	Pot	No data	Reduced Cd accumulation by 85.9~87.5%	Reduce the mobility and plant availability of Cd, alleviated oxidative stress & phytotoxicity	[18]
Pak choi	Surface layer of farmland	bamboo biochar (600 °C), rice straw Biochar (600 °C)	0.5%, 1%, 2.5%, 5%	Pot	8.70	Reduced Cd accumulation by 17.0~35.4%	Promote the conversion of Cd into insoluble precipitates such as hydroxides, carbonates, phosphates, etc.	[47]

Table 3. *Cont.*

Crop	Soil Type	Biochar Feedsock (PyrolysisTemp.)	Dose (*w*/*w*)	Exp.Setup	Initial Soil Cd (mg/kg)	Cd Reduction in Edible Tissue	Growth Response/ Mechanisms	Ref.
Pak choi	Alfisol	rice-straw (550 °C)	2.5%, 5%	Pot	1.422	Reduced Cd accumulation by 42.49%	Alleviated oxidative stress & phytotoxicity	[48]
Brassica rapa	Pb Cd composite polluted soil	Coconut-husk + nZVI (800 °C)	0.025%, 0.05%	Pot	2.43	Reduced Pb/Cd accumulation by 32.4–77.9%	Enhanced plant growth and photosynthesis/Alleviated oxidative stress,	[49]
Red & Green amaranth	Cultivated soil contaminated Cd	Tobacco straw (360 °C)	1%, 2%, 5%	Pot	2.18	Red: Reduced by 18.5~37.6% Green: 4.6~11.8%	Cultivar-specific: Red: Promoted biomass Green: Inhibited plant growth	This study

4.3. The Interplay Between Soil Cd Bioavailability, Plant Performance, and Accumulation Mitigation

The factorial experimental design in the present study clearly highlights the divergent responses of the red and green amaranth cultivars to Cd accumulation under biochar amendment. The highly significant interaction (Biochar × Cultivar) observed for Shoot Cd, Root Cd, and BCF ($p < 0.001$, Figure 3) confirms that the efficacy of biochar in regulating Cd uptake is highly cultivar-dependent. For red amaranth, soil exchangeable Cd was significantly and positively correlated with shoot Cd and BCF, but negatively correlated with key growth indicators (biomass, plant height) and Pn (Figure 6). We speculated a linear mechanistic pathway: biochar application effectively reduces exchangeable Cd (immobilization) → limits plant Cd uptake → alleviates Cd-induced phytotoxicity → preserves physiological function (Pn) → ultimately enhances biomass accumulation. Thus, for the red cultivar, biochar functions synergistically as both a soil remediation agent and a plant growth promoter. In contrast, the mechanistic interplay in green amaranth was more intricate and somewhat paradoxical. While biochar successfully curtailed its Cd accumulation, the exchangeable Cd concentration in the soil was actually positively correlated with shoot fresh weight (Figure 6). This relationship contradicts standard toxicological principles (where lower Cd should yield higher biomass) and implies the presence of a dominant, secondary stressor limiting its growth. The pronounced growth inhibition of the green cultivar under the 5% biochar treatment indicates a non-linear, dose-dependent response. This phenomenon is likely driven by biochar-induced nutrient immobilization and altered soil-root dynamics. High application rates of biochar can release excessive dissolved organic carbon (DOC) and elevate soil pH, which may temporarily complex with or precipitate essential micronutrients, leading to nutrient imbalance [50,51].

Although the basal fertilization was strictly standardized across all treatments, the biochar itself acted as a massive source of exogenous nutrients, which fundamentally altered the rhizosphere chemistry at higher application rates. Based on our basal fertilization protocol, the standard nutrient supply provided approximately 124.5 mg of elemental K per pot. However, the tobacco straw-derived biochar contained an inherently high level of available K (60,648 mg/kg, Table 1). Specifically, the 1%, 2%, and 5% biochar treatments introduced approximately 303 mg, 606 mg, and 1516 mg of available K per pot, respectively. This indicates that the potassium content provided by applying 5% biochar treatment is more than 13 times that of the standard basal fertilization amount, and the 2% treatment also reaches nearly 5 times. Theoretically, an excessively high concentration of monovalent K^+ in the soil solution inevitably induces severe cation antagonism, aggressively competing with and inhibiting the root uptake of other essential divalent cations, particularly Ca^{2+} and Mg^{2+} [52,53]. We postulate that this dramatic nutrient imbalance, exacerbated by high K/Mg ratios, impairs critical physiological processes such as photosynthesis and cell

elongation [54]. Furthermore, the trend of changes in electrical conductivity (EC) between two cultivars also reflects the fundamental different soil–root dynamics (Figure 2B). In the red cultivar, soil EC decreased dose-dependently, aligning with its robust biomass accumulation and active root uptake of dissolved ions. Conversely, under the 5% treatment, the EC of the green cultivar's soil spiked dramatically (1.77 times higher than the CK). While the EC value remains below the threshold for severe osmotic salt stress, this localized accumulation of soluble salts physically proves that the nutrient uptake capacity of the green amaranth roots was severely compromised. We hypothesize that biochar-induced cationic antagonism caused a cessation of ion absorption, leading to the abnormal accumulation of biochar-derived salts in the rhizosphere. However, the absence of direct quantification for DOC and specific root exudate profiles, coupled with the lack of total nitrogen (TN) data for both the biochar and soil, precludes a clear understanding of temporal shifts in nitrogen availability and its specific role in the plant growth response. Consequently, this limitation prevents a comprehensive nitrogen balance assessment within the soil-plant-biochar system. Therefore, our proposed stress-based interpretation remains largely hypothetical at this stage. Future research must explicitly quantify these parameters to transition from empirical observations to a fully validated mechanistic model.

4.4. Limitations and Future Perspectives

This study validates the efficacy of tobacco straw-derived biochar in securing the safe production of leafy vegetables in Cd-contaminated soils by driving Cd speciation towards stable fractions. Crucially, it reveals that the net agricultural outcome is a composite result of alleviated heavy metal toxicity and biochar-induced microenvironmental shifts, with plant genotype acting as the definitive factor determining whether this remediation strategy enhances or compromises crop yield. While this study provides valuable mechanistic insights into cultivar-specific responses to biochar, several limitations must be acknowledged. The 30-day pot experiment with a small soil volume (500 g) does not capture the long-term aging effects of biochar, complex rhizosphere dynamics under field conditions, or seasonal climatic variability. The lack of precise particle size distribution also limits the physio-chemical interpretation of soil-biochar interactions. Therefore, extrapolating these greenhouse findings to large-scale agricultural practice requires caution, and extensive long-term field validations are imperative. Several critical methodological limitations also constrain the full mechanistic interpretation of these findings. Firstly, the absence of S_{BET} for the biochar limits our ability to definitively model the physical sorption mechanisms of Cd. Secondly, the lack of complete elemental profiling, particularly Total Nitrogen in both the biochar and soil, prevents a comprehensive nitrogen balance assessment, meaning that temporary nutrient immobilization or altered nitrogen dynamics cannot be unequivocally excluded as factors influencing plant growth. Additionally, while the observed growth inhibition in green amaranth at high biochar doses was hypothesized to be related to root-zone microenvironment disruptions (such as DOC fluxes), the lack of direct DOC measurements renders this explanation partially speculative. Finally, due to the unsuitability of the Walkley–Black method for biochar matrices, accurate true carbon content was excluded. Therefore, the mechanistic framework proposed herein should be viewed as an exploratory synthesis. Future research must incorporate rigorous elemental analysis, precise soil granulometry, and dynamic DOC tracking to move beyond empirical observations toward a fully verified, data-driven mechanistic model.

5. Conclusions

This study demonstrates that tobacco straw-derived biochar is a highly effective agricultural amendment for the in-situ immobilization of cadmium (Cd) and the mitigation of its accumulation in leafy vegetables. Mechanistically, biochar application elevated soil pH and drove the transformation of highly bioavailable exchangeable Cd into the more stable Fe-Mn oxide-bound fraction. Consequently, this microenvironmental shift significantly suppressed Cd uptake in both tested amaranth cultivars, as evidenced by marked reductions in tissue Cd concentrations and BCF. Crucially, the agronomic efficacy of the biochar was highly dose-dependent and species-specific. For the red amaranth cultivar, a 2% (*w*/*w*) application rate emerged as the optimal strategy, concurrently maximizing the reduction in shoot Cd accumulation (by 37.6%) and promoting substantial biomass expansion (a 58.6% increase in shoot dry weight). Conversely, while biochar successfully limited Cd uptake in the green amaranth cultivar, it concomitantly induced varying degrees of growth inhibition, highlighting a potential physiological trade-off.

In conclusion, the 2% biochar application is highly effective for the red cultivar, bringing its edible tissue Cd concentration down to the regulatory food safety limit (0.2 mg/kg FW), significantly reducing health risks. However, considering the short-term and greenhouse-based nature of this study, extensive field-scale trials, long-term stability assessments of Cd immobilization, and validations based on fresh-weight food safety limits are imperative before generalizing this optimal application rate to broader agricultural practice.

Author Contributions: J.L.: Writing—original draft, Investigation, Data curation, Conceptualization. S.Z.: Writing—review and editing, Data curation. Z.M.: Investigation. G.D.: Investigation. Y.L.: Supervision. M.D.: Supervision. J.G.: Writing—review and editing, Data curation. J.Z.: Writing—review and editing, Resources, Funding acquisition, Conceptualization. All authors have read and agreed to the published version of the manuscript.

Funding: This research was supported by the earmarked fund for China Agriculture Research System (CARS-21) and Yunnan Provincial Science and Technology Plan Project (202204BI090004).

Data Availability Statement: The original contributions presented in this study are included in the article. Further inquiries can be directed to the corresponding authors.

Conflicts of Interest: The authors declare no conflicts of interest.

References

1. Tchounwou, P.; Yedjou, C.; Patlolla, A.; Sutton, D. Heavy metal toxicity and the environment. In *Molecular, Clinical and Environmental Toxicology*; Luch, A., Ed.; Springer: Basel, Switzerland, 2012; Volume 101, pp. 133–164, Experientia Supplementum. [CrossRef] [PubMed]
2. Huang, K.; Lin, L.; Liao, M.; Liu, J.; Liang, D.; Xia, H.; Wang, X.; Wang, J.; Deng, H. Effects of intercropping with different Solanum plants on the physiological characteristics and cadmium accumulation of *Solanum nigrum*. *Int. J. Environ. Anal. Chem.* **2020**, *101*, 2835–2847. [CrossRef]
3. Xu, Z.; Wang, D.; Tang, W.; Wang, L.; Li, Q.; Lu, Z.; Liu, H.; Zhong, Y.; He, T.; Guo, S. Phytoremediation of cadmium-polluted soil assisted by D-gluconate-enhanced Enterobacter cloacae colonization in the *Solanum nigrum* L. rhizosphere. *Sci. Total Environ.* **2020**, *732*, 139265. [CrossRef] [PubMed]
4. Xu, Z.; Lu, Z.; Zhang, L.; Fan, H.; Wang, Y.; Li, J.; Lin, Y.; Liu, H.; Guo, S.; Xu, M.; et al. Red mud based passivator reduced Cd accumulation in edible amaranth by influencing root organic matter metabolism and soil aggregate distribution. *Environ. Pollut.* **2021**, *275*, 116543. [CrossRef] [PubMed]
5. Gholizadeh, M.; Hu, X. Removal of heavy metals from soil with biochar composite: A critical review of the mechanism. *J. Environ. Chem. Eng.* **2021**, *9*, 105830. [CrossRef]
6. Zhu, Z.; Zhang, Y.; Tao, W.; Zhang, X.; Xu, Z.; Xu, C. The biological effects of biochar on soil's physical and chemical characteristics: A review. *Sustainability* **2025**, *17*, 2214. [CrossRef]

7. Hossain, M.; Bahar, M.; Sarkar, B.; Donne, S.; Ok, Y.; Palansooriya, K.; Kirkham, M.; Chowdhury, S.; Bolan, N. Biochar and its importance on nutrient dynamics in soil and plant. *Biochar* **2020**, *2*, 379–420. [CrossRef]
8. Wang, Y.; Shen, X.; Bian, R.; Liu, X.; Zheng, J.; Cheng, K.; Xuhui, Z.; Li, L.; Pan, G. Effect of pyrolysis temperature of biochar on Cd, Pb and As bioavailability and bacterial community composition in contaminated paddy soil. *Ecotoxicol. Environ. Saf.* **2022**, *247*, 114237. [CrossRef] [PubMed]
9. Yan, S.; Zhang, S.; Yan, P.; Aurangzeib, M. Effect of biochar application method and amount on the soil quality and maize yield in Mollisols of Northeast China. *Biochar* **2022**, *4*, 56. [CrossRef]
10. Mansoor, S.; Kour, N.; Manhas, S.; Zahid, S.; Wani, O.; Sharma, V.; Wijaya, L.; Alyemeni, M.; Alsahli, A.; El-Serehy, H.; et al. Biochar as a tool for effective management of drought and heavy metal toxicity. *Chemosphere* **2021**, *271*, 129458. [CrossRef] [PubMed]
11. Medha, I.; Chandra, S.; Vanapalli, K.; Samal, B.; Bhattacharya, J.; Das, B. (3-Aminopropyl)triethoxysilane and iron rice straw biochar composites for the sorption of Cr (VI) and Zn (II) using the extract of heavy metals contaminated soil. *Sci. Total Environ.* **2021**, *771*, 144764. [CrossRef] [PubMed]
12. Wang, H.; Huang, F.; Zhao, Z.; Wu, R.; Xu, W.; Wang, P.; Xiao, R. High-efficiency removal capacities and quantitative adsorption mechanisms of Cd^{2+} by thermally modified biochars derived from different feedstocks. *Chemosphere* **2021**, *272*, 129594. [CrossRef] [PubMed]
13. Li, J.; Song, M.; Yin, J.; Fenton, O.; Gao, L.; Tian, Y. The beneficial effects of biochar on overall soil quality and plant performance are dose-dependent and are closely associated with soil pH. *Pedosphere* **2025**. [CrossRef]
14. Tan, Z.; Yuan, S.; Hong, M.; Zhang, L.; Huang, Q. Mechanism of negative surface charge formation on biochar and its effect on the fixation of soil Cd. *J. Hazard. Mater.* **2020**, *384*, 121370. [CrossRef] [PubMed]
15. Zhang, R.; Li, Z.; Liu, X.; Wang, B.; Zhou, G.; Huang, X.; Lin, C.; Wang, A.; Brooks, M. Immobilization and bioavailability of heavy metals in greenhouse soils amended with rice straw-derived biochar. *Ecol. Eng.* **2017**, *98*, 183–188. [CrossRef]
16. Chen, K.; Pai, C.; Lai, H. Amendment of Husk Biochar on Accumulation and Chemical Form of Cadmium in Lettuce and Pak-Choi Grown in Contaminated Soil. *Water* **2020**, *12*, 868. [CrossRef]
17. Coumar, M.V.; Parihar, R.S.; Dwivedi, A.K.; Saha, J.K.; Rajendiran, S.; Dotaniya, M.L.; Kundu, S. Impact of pigeon pea biochar on cadmium mobility in soil and transfer rate to leafy vegetable spinach. *Environ. Monit. Assess.* **2016**, *188*, 31. [CrossRef] [PubMed]
18. Wang, J.; Cai, R.; Hu, Z.; Cai, L.; Wu, J. Study on the Interaction Effect of Heavy Metal Cadmium in Soil–Plant System Controlled by Biochar and Nano-Zero-Valent Iron. *Int. J. Mol. Sci.* **2025**, *26*, 4373. [CrossRef] [PubMed]
19. Chen, S.; Ye, Y.; Liao, F.; Wu, S.; Zhang, K. Insight into the uptake, translocation, metabolism, dissipation and risk assessment of tolfenpyrad in romaine and edible amaranth grown in hydroponic conditions. *Food Chem.* **2024**, *437*, 137896. [CrossRef] [PubMed]
20. He, B.; Yu, D.; Chen, Y.; Shi, J.; Xia, Y.; Li, Q.; Wang, L.; Ling, L.; Zeng, E. Use of low-calcium cultivars to reduce cadmium uptake and accumulation in edible amaranth (*Amaranthus mangostanus* L.). *Chemosphere* **2017**, *171*, 588–594. [CrossRef] [PubMed]
21. Roy, R.; Hossain, A.; Sultana, S.; Deb, B.; Ahmod, M.M.; Sarker, T. Microplastics increase cadmium absorption and impair nutrient uptake and growth in red amaranth (*Amaranthus tricolor* L.) in the presence of cadmium and biochar. *BMC Plant Bio* **2024**, *24*, 608. [CrossRef] [PubMed]
22. *GB 15618-2018*; Soil Environmental Quality—Risk Control Standard for Soil Contamination of Agricultural Land. Ministry of Ecology and Environment of the People's Republic of China: Beijing, China, 2018.
23. *GB 5009.268-2016*; National Food Safety Standard—Determination of Multiple Elements in Foods. National Health and Family Planning Commission of the People's Republic of China: Beijing, China, 2016.
24. *HJ 1315-2023*; Soil and Sediment—Determination of Metal Elements. Ministry of Ecology and Environment of the People's Republic of China: Beijing, China, 2023.
25. *GB/T 25282-2010*; Soil and Sediment—Sequential Extraction Procedure for the Speciation of 13 Trace Elements. Standardization Administration of the People's Republic of China: Beijing, China, 2010.
26. Omokaro, G.; Kornev, K.; Nafula, Z.; Chikukula, A.; Osayogie, O.; Efeni, O. Biochar for sustainable soil management: Enhancing soil fertility, plant growth and climate resilience. *Farming Syst.* **2025**, *3*, 100167. [CrossRef]
27. Gong, X.; Huang, D.; Liu, Y.; Zeng, G.; Wang, R.; Wei, J.; Huang, C.; Xu, P.; Wan, J.; Zhang, C. Pyrolysis and reutilization of plant residues after phytoremediation of heavy metals contaminated sediments: For heavy metals stabilization and dye adsorption. *Bioresour. Technol.* **2018**, *253*, 64–71. [CrossRef] [PubMed]
28. Lawrinenko, M.; Laird, D.; Johnson, R.; Jing, D. Accelerated aging of biochars: Impact on anion exchange capacity. *Carbon* **2016**, *103*, 217–227. [CrossRef]
29. Leng, L.; Huang, H.; Li, H.; Li, J.; Zhou, W. Biochar stability assessment methods: A review. *Sci. Total Environ.* **2019**, *647*, 210–222. [CrossRef] [PubMed]

30. Boostani, H.; Hosseini, S.; Hardie, A. Mechanisms of Cd immobilization in contaminated calcareous soils with different textural classes treated by acid- and base-modified biochars. *Sci. Rep.* **2024**, *14*, 24614. [CrossRef] [PubMed]
31. Ge, S.; Zhao, S.; Wang, L.; Zhao, Z.; Wang, S.; Tian, C. Exploring adsorption capacity and mechanisms involved in cadmium removal from aqueous solutions by biochar derived from euhalophyte. *Sci. Rep.* **2024**, *14*, 450. [CrossRef] [PubMed]
32. Tomczyk, A.; Sokołowska, Z.; Boguta, P. Biochar physicochemical properties: Pyrolysis temperature and feedstock kind effects. *Rev. Environ. Sci. Biotechnol.* **2020**, *19*, 191–215. [CrossRef]
33. Li, H.; Dong, X.; da Silva, E.B.; de Oliveira, L.M.; Chen, Y.; Ma, L.Q. Mechanisms of metal sorption by biochars: Biochar characteristics and modifications. *Chemosphere* **2017**, *178*, 466–478. [CrossRef] [PubMed]
34. Zhang, N.; Xing, J.; Wei, L.; Liu, C.; Zhao, W.; Liu, Z.; Wang, Y.; Liu, E.; Ren, X.; Jia, Z.; et al. The potential of biochar to mitigate soil acidification: A global meta-analysis. *Biochar* **2025**, *7*, 49. [CrossRef]
35. Bian, R.; Chen, D.; Liu, X.; Cui, L.; Li, L.; Pan, G.; Xie, D.; Zheng, J.; Zhang, X.; Zheng, J.; et al. Biochar soil amendment as a solution to prevent Cd-tainted rice from China: Results from a cross-site field experiment. *Ecol. Eng.* **2013**, *58*, 378–383. [CrossRef]
36. Zheng, R.; Chen, Z.; Cai, C.; Tie, B.; Liu, X.; Reid, B.; Huang, Q.; Lei, M.; Sun, G.; Baltrėnaitė, E. Mitigating heavy metal accumulation into rice (*Oryza sativa* L.) using biochar amendment—A field experiment in Hunan, China. *Environ. Sci. Pollut. Res.* **2015**, *22*, 11097–11108. [CrossRef] [PubMed]
37. Xu, P.; Sun, C.; Ye, X.; Xiao, W.; Zhang, Q.; Wang, Q. The effect of biochar and crop straws on heavy metal bioavailability and plant accumulation in a Cd and Pb polluted soil. *Ecotoxicol. Environ. Saf.* **2016**, *132*, 94–100. [CrossRef] [PubMed]
38. Zhang, C.; Wang, W.; Duan, A.; Zeng, G.; Huang, D.; Lai, C.; Tan, X.; Cheng, M.; Wang, R.; Zhou, C.; et al. Adsorption behavior of engineered carbons and carbon nanomaterials for metal endocrine disruptors: Experiments and theoretical calculation. *Chemosphere* **2019**, *222*, 184–194. [CrossRef] [PubMed]
39. Chi, K.; Fan, H. Characteristics of Cd uptake and translocation in two cultivars of Amaranth (*Amaranthus mangostanus* L.). *J. Plant Nutr. Fertil.* **2016**, *22*, 1612–1619. (In Chinese) [CrossRef]
40. Fan, H.; Zhou, W. Screening of amaranth cultivars (*Amaranthus mangostanus* L.) for cadmium hyperaccumulation. *Agric. Sci. China* **2009**, *8*, 342–351. [CrossRef]
41. Emam, T.; Hosni, A.; Ismail, A.; El-Kinany, R.; Hewidy, M.; Saudy, H.; Omar, M.; Ibrahim, M.; Sui, S.; El-Sayed, S. Physiological and molecular responses of red amaranth (*Amaranthus cruentus* L.) and green amaranth (*Amaranthus hypochondriacus* L.) to salt stress. *J. Soil Sci. Plant Nutr.* **2025**, *25*, 171–182. [CrossRef]
42. Lu, Z.; Wang, X.; Lin, X.; Mostafa, S.; Zou, H.; Wang, L.; Jin, B. Plant anthocyanins: Classification, biosynthesis, regulation, bioactivity, and health benefits. *Plant Physiol. Biochem.* **2024**, *217*, 109268. [CrossRef] [PubMed]
43. Ai, Y.; Wang, Y.; Song, L.; Hong, W.; Zhang, Z.; Li, X.; Zhou, S.; Zhou, J. Effects of biochar on the physiology and heavy metal enrichment of Vetiveria zizanioides in contaminated soil in mining areas. *J. Hazard. Mater.* **2023**, *448*, 130965. [CrossRef] [PubMed]
44. Murtaza, G.; Ahmed, Z.; Usman, M.; Tariq, W.; Ullah, Z.; Shareef, M.; Lqbal, H.; Waqas, M.; Tariq, A.; Wu, Y.; et al. Biochar induced modifications in soil properties and its impacts on crop growth and production. *J. Plant Nutr.* **2021**, *44*, 1677–1691. [CrossRef]
45. Liu, S.; Cen, B.; Yu, Z.; Qiu, R.; Gao, T.; Long, X. The key role of biochar in amending acidic soil: Reducing soil acidity and improving soil acid buffering capacity. *Biochar* **2025**, *7*, 52. [CrossRef]
46. Zhao, Z.; Chen, J.; Gao, S.; Lu, T.; Li, L.; Farooq, U.; Gang, S.; Lv, M.; Qi, Z. Low-molecular-weight aromatic acids mediated the adsorption of Cd^{2+} onto biochars: Effects and mechanisms. *Environ. Sci. Pollut. Res.* **2024**, *31*, 15597–15610. [CrossRef] [PubMed]
47. Liu, Y.; Wang, Y.; Lu, H.; Lonappan, L.; Brar, S.K.; He, L.; Chen, J.; Yang, S. Biochar application as a soil amendment for decreasing cadmium availability in soil and accumulation in *Brassica chinensis*. *J. Soils Sediments* **2018**, *18*, 2511–2519. [CrossRef]
48. Kamran, M.; Malik, Z.; Parveen, A.; Zong, Y.; Abbasi, G.H.; Rafiq, M.T.; Shaaban, M.; Mustafa, A.; Bashir, S.; Rafay, M.; et al. Biochar alleviates Cd phytotoxicity by minimizing bioavailability and oxidative stress in pak choi (*Brassica chinensis* L.) cultivated in Cd-polluted soil. *J. Environ. Manag.* **2019**, *250*, 109500. [CrossRef] [PubMed]
49. Aborisade, M.A.; Geng, H.; Oba, B.T.; Kumar, A.; Ndudi, E.A.; Battamo, A.Y.; Liu, J.; Chen, D.; Okimiji; O.P. Ojekunle, O.Z.; et al. Remediation of soil polluted with Pb and Cd and alleviation of oxidative stress in *Brassica rapa* plant using nanoscale zerovalent iron supported with coconut-husk biochar. *J. Plant Physiol.* **2023**, *288*, 154023. [CrossRef] [PubMed]
50. Joseph, S.; Cowie, A.L.; Zwieten, L.V.; Bolan, N.; Budai, A.; Buss, W.; Cayuela, M.L.; Graber, E.R.; Ippolito, J.A.; Kuzyakov, Y.; et al. How biochar works, and when it doesn't: A review of mechanisms controlling soil and plant responses to biochar. *Glob.* **2021**, *27*, 4124–4145. [CrossRef] [PubMed]
51. Singh, E.; Kumar, A.; Mishra, R.; You, S.; Singh, L.; Kumar, S.; Kumar, R. Pyrolysis of waste biomass and plastics for production of biochar and its use for removal of heavy metals from aqueous solution. *Bioresour. Technol.* **2020**, *320*, 124278. [CrossRef] [PubMed]
52. Marschner, P. *Marschner's Mineral Nutrition of Higher Plants*, 3rd ed.; Academic Press: Cambridge, MA, USA, 2012. [CrossRef]

53. Pantha, P.; Oh, D.-H.; Longstreth, D.; Dassanayake, M. Living with high potassium: Balance between nutrient acquisition and K-induced salt stress signaling. *Plant Physiol.* **2023**, *191*, 1102–1121. [CrossRef] [PubMed]
54. Gransee, A.; Führs, H. Magnesium mobility in soils as a challenge for soil and plant analysis, magnesium fertilization and root uptake under adverse growth conditions. *Plant Soil* **2013**, *368*, 5–21. [CrossRef]

Disclaimer/Publisher's Note: The statements, opinions and data contained in all publications are solely those of the individual author(s) and contributor(s) and not of MDPI and/or the editor(s). MDPI and/or the editor(s) disclaim responsibility for any injury to people or property resulting from any ideas, methods, instructions or products referred to in the content.